

# Generating Neural Networks with Neural Networks

Lior Deutsch  
 sliorde@gmail.com

January 2018

## Abstract

Hypernetworks are neural networks that transform a random input vector into weights for a specified target neural network. We formulate the hypernetwork training objective as a compromise between accuracy and diversity, where the diversity takes into account trivial symmetry transformations of the target network. We show that this formulation naturally arises as a relaxation of an optimistic probability distribution objective for the generated networks, and we explain how it is related to variational inference. We use multi-layered perceptrons to form the mapping from the low dimensional input random vector to the high dimensional weight space, and demonstrate how to reduce the number of parameters in this mapping by weight sharing. We perform experiments on a four layer convolutional target network which classifies MNIST images, and show that the generated weights are diverse and have interesting distributions.

## 1 Introduction

Generating high quality samples from hierarchical and high dimensional probability distributions has been an ongoing research area for decades now. The rise of deep learning in recent years has led to the emergence of various new methods, such as the Variational Autoencoder(VAE)[1] and the Generative Adversarial Network(GAN)[2], which are able to synthesize impressive samples after being trained on large and complex data sets, including images[2], video[3], text[4], molecules[5] and more. The training of these generative models is data driven, and an essential requirement is the existence of a rich enough data set, which represents well the underlying probability distribution. A trained VAE decoder or GAN works by feeding it with a (usually random) input vector, and it typically generates the output sample in a single forward pass, in  $\mathcal{O}(1)$  time.

It is natural to suggest that these generative methods be used for the generation of the weights of a neural network<sup>1</sup> of a given target architecture. After all, just like images and videos, a neural network is a structured array of numbers. Indeed, recent works[6, 7] have presented neural networks that, once trained, are operated similarly to GANs and VAE decoders, by transforming a random

---

<sup>1</sup>By “weights” we are referring to any trainable parameter of a neural network, including bias parameters

input vector into a sample of the weights of another neural network. The term *hypernetwork*[8, 6] was coined for the former type of network. The goal of generating weights for a neural network with a given target architecture differs from the previously mentioned applications of generative methods, since a hypernetwork cannot be trained in a data driven manner in the same sense. The reason is that there is no rich data set of neural networks for each given target architecture and each task, and it can be quite expensive to create such a data set. This means that we cannot train a hypernetwork using the same methods mentioned above, and that it's not useful to talk about an existing probability distribution of neural networks. In the absence of a probability distribution, we take a different approach, where we decide upon certain useful properties that such a distribution would have, express them as loss function terms, and train the hypernetwork so as to optimize the loss function. The two useful properties are **accuracy** and **diversity**. The former implies that the generated neural networks achieve high accuracy in performing their intended tasks. The diversity property means that the hypernetwork could generate a big number of *essentially different* networks.

Previous works[6, 7] are set up in a Bayesian context. Using variational inference, they find an approximation to the posterior distribution of the weights  $\theta$ . A key ingredient is that the target network outputs probabilities  $p(x|\theta)$  (e.g. softmax in classification networks), and for a data set  $D = \{x_1, x_2, \dots\}$ ,  $p(D|\theta) = p(x_1|\theta)p(x_2|\theta)\dots$ . This, together with a prior  $p(\theta)$ , uniquely determines the posterior  $p(\theta|D)$  via Bayes' theorem  $\log p(\theta|D) = \log p(D|\theta) + \log p(\theta) - \log Z$  for a normalizing factor  $Z$ . The underlying assumption is that the network  $p(x|\theta)$  and the prior  $p(\theta)$  jointly form a generative model of the data. In other words, the probabilities  $p(x|\theta)$  are viewed as “true”, and therefore they can be plugged into Bayes' formula. The result is that the objective function in hypernetwork variational inference does not have any explicit hyperparameter that expresses the quality of the model  $p(x|\theta)$ . A simple correction to Bayes' law would be to view the networks' output probabilities as mere approximations  $\hat{p}(x|\theta)$ , and then the formula takes the form  $\log p(\theta|D) = \lambda \log \hat{p}(D|\theta) + \log p(\theta) - \log Z$ , and the hyperparameter  $\lambda$  would also appear in the variational inference objective. In the current paper, we do not take a Bayesian viewpoint, which allows us to apply the framework to any kind of target network, even if it does not compute probabilities. The hyperparameter  $\lambda$  arises as a compromise between accuracy and diversity. And we allow the diversity loss component to take forms other than entropy, which is what is used in variational inference. In particular, we show how to make the diversity more meaningful by taking into account symmetry transformations, such as scaling, whose operation should not be considered as contributing to the diversity.

In section 2 we describe the loss function that we use for hypernetwork training, and show how it arises as a relaxation of an optimistic objective. Then, we explain how we incorporate symmetry considerations into the diversity term, and we describe the architecture for the hypernetwork. In section 3 we discuss related work, and then in section 4 we describe experiments and their results. We conclude with section 5, where we supply additional thoughts about the hypernetwork framework.

## 2 Methods

### 2.1 Hypernetworks

Let  $T(x; \theta) : X \times \Theta \rightarrow Y$  be a parametric function approximator, where  $X$  is the input domain,  $Y$  is the output domain and  $\Theta$  is the parameter space. We will focus in particular on  $T$  being a neural network for classification of images with  $n$  classes, thus  $X$  is a set of images, and  $Y \subset \mathbb{R}^n$  is the set of probability distributions over the set of classes.  $\Theta$  is the set of trainable weight vectors of the network. We refer to  $T$  as the *target network architecture*, or more shortly as the *target network*. The standard supervised learning approach for obtaining weights  $\theta$  that yield good classification performance is to choose an appropriate loss function  $\mathcal{L}(\theta | p_{\text{data}}(x, y))$ , where  $p_{\text{data}}(x, y)$  is the data distribution, and to minimize it over the weights  $\theta$  via backpropagation, where the loss function gradients are estimated using batches of samples from the training data set. The result is an optimal vector of weights  $\theta^*$ . The set of possible results may be very large, due to three reasons: **(a)** The prevalence of local minima and flat regions in the loss function surface[9, 10]; **(b)** Discrete symmetry transformations, such as permutation between filters, and continuous symmetry transformations, such as scaling, which keep the network output unchanged; **(c)** The finite nature of the backpropagation algorithm (finite learning rate, finite number of steps and finite precision in calculations).

The hypernetwork approach is different. Instead of obtaining  $\theta^*$  by directly minimizing  $\mathcal{L}$  over the weights  $\theta$ , we obtain  $\theta^*$  as the output of a generator function  $G(z) : Z \rightarrow \Theta$ , where  $Z$  is some input domain. We will draw the values for  $z$  from a simple probability distribution  $p_{\text{noise}}$ , thus making  $G(z)$  random. We use a parametric representation for  $G$ , and choose it to be a neural network  $G(z; \varphi) : Z \times \Phi \rightarrow \Theta$ , where  $\Phi$  is the space of parameters<sup>2</sup> of the network  $G$ . We will occasionally use the notation  $G(z)$  to refer to  $G(z; \varphi)$ . We refer to  $G$  as a *hypernetwork*.  $G$  must be trained so that parameters  $\varphi^*$  are found which yield suitable weights  $G(z; \varphi^*)$  for the target network with a high probability. In other words, the objective is to optimize over  $\varphi$  in the combined network  $T(x; G(z; \varphi))$ , so that with high probability we get low values of  $\mathcal{L}$ .

### 2.2 Objective Function

To get benefits from having a trained hypernetwork, it is not enough that  $T(x; G(z; \varphi^*))$  performs well as a classifier. It is also important that different values of  $z$  yield essentially different networks  $\theta \in \Theta$ . This forces us to let the hypernetwork  $G(z)$  generate also sub-optimal weights, since as a continuous function its image cannot contain only optimal weights without a continuous path in weight space between them. A non-formal definition of “essentially different” is: two weight vectors  $\theta_1, \theta_2 \in \Theta$  are considered essentially different if there is no trivial symmetry transformation that transforms  $\theta_1$  into a close proximity of  $\theta_2$ , where the proximity is the norm of the difference  $\theta_1 - \theta_2$ . Symmetry transformations are functions  $S : \Theta \rightarrow \Theta$  such that  $T(x; \theta) = T(x; S(\theta))$  for all  $x \in X$  and all  $\theta \in \Theta$ . The trivial symmetry transformations include:

1. **Scaling** - If the target network is a feed-forward convolutional network

---

<sup>2</sup>To reduce confusion, we refer to  $\theta$  as “weights” and to  $\varphi$  as “parameters”.

with piecewise-linear activations such as ReLU[11, 12] or leaky-ReLU[13], then scaling of the weights of one filter<sup>3</sup> by a positive factor, while unscaling the weights of all filters in the corresponding channel in the next layer by the same factor, keeps the output of the network unchanged.

2. **Logits' bias** - If a network produces logit values which are fed into a softmax layer, then adding the same number to all logit values does not change the values of the softmax probabilities.
3. **Permutation** - Permuting the filters in a layer while performing the same permutation on the channels of the filters in the next layer.
4. **Composition** - Any composition of the previous symmetry transformations.

Thus, we train  $G$  by minimizing over a loss function which includes two terms:

$$L(\varphi|p_{\text{noise}}, p_{\text{data}}) = \lambda L_{\text{accuracy}}(\varphi|p_{\text{noise}}, p_{\text{data}}) + L_{\text{diversity}}(\varphi|p_{\text{noise}}), \quad (1)$$

where  $L_{\text{accuracy}}$  depends on  $\mathcal{L}$ . An obvious choice for  $L_{\text{accuracy}}$  is

$$L_{\text{accuracy}} = \mathbb{E}_{z \sim p_{\text{noise}}} \mathcal{L}(G(z; \varphi) | p_{\text{data}}). \quad (2)$$

$L_{\text{diversity}}$  should ensure that there is high diversity in the results of  $G$  as a function of  $z$ , taking into account the trivial symmetry transformations.  $\lambda > 0$  is a hyperparameter that balances the two losses.

At this point we can choose the functions  $L_{\text{accuracy}}$  and  $L_{\text{diversity}}$ , but we first wish to demonstrate how this form of loss function arises from another consideration. We denote by  $p_{\varphi}(\theta)$  the probability distribution over  $\Theta$  of  $\theta = G(z; \varphi)$ . We also denote by  $p(\theta|p_{\text{data}})$  the required distribution over  $\Theta$ , which we would like  $p_{\varphi}(\theta)$  to be equal to. An optimistic choice for  $p(\theta|p_{\text{data}})$  would be the following:

$$p(\theta|p_{\text{data}}) = \begin{cases} \frac{1}{Z} & \text{if } \mathcal{L}(\theta|p_{\text{data}}) = \min_{\theta'} \mathcal{L}(\theta'|p_{\text{data}}) \\ 0 & \text{otherwise} \end{cases} \quad (3)$$

where  $Z$  is a normalization constant. In other words, this distribution chooses only from the global optima, with equal probabilities. We can relax this optimistic form by turning it into a Gibbs distribution:

$$p(\theta|p_{\text{data}}) = \frac{\exp(-\lambda \mathcal{L}(\theta|p_{\text{data}}))}{Z}, \quad (4)$$

The hyperparameter  $\lambda > 0$  controls how close this distribution is to the optimistic form, which is recovered for  $\lambda \rightarrow \infty$ . The relaxation is required so that there is higher connectivity between the mode regions of  $p(\theta|p_{\text{data}})$ . This will make it possible for  $p_{\varphi}(\theta)$  to become close to  $p(\theta|p_{\text{data}})$ . Making  $p_{\varphi}(\theta)$  close to  $p(\theta|p_{\text{data}})$  can be done by minimizing a loss function which is the Kullback-Leibler divergence between them:

---

<sup>3</sup>In our context, the weights at the input of a neuron in a fully connected layer are also considered a filter, whose receptive field is the entire previous layer.

$$L = D_{\text{KL}}(p_\varphi(\theta) \| p(\theta|p_{\text{data}})) = \int p_\varphi(\theta) \log \left( \frac{p_\varphi(\theta)}{p(\theta|p_{\text{data}})} \right) d\theta. \quad (5)$$

This integral can be defined also when  $p_\varphi(\theta)$  is supported on a low dimensional manifold<sup>4</sup>. Inserting (4) into (5) we get:

$$L = \lambda \mathbb{E}_{\theta \sim p_\varphi} \mathcal{L}(\theta|p_{\text{data}}) + \mathbb{E}_{\theta \sim p_\varphi} \log p_\varphi(\theta) + \log Z, \quad (6)$$

Noticing that  $\log Z$  is a constant (does not depend on  $p_\varphi$ ), we see that (6) is of the form of (1), where the diversity term is taken as the negation of the (differential) entropy. It is not surprising that the entropy can behave as diversity term.

The appearance of the entropy in (6) is a result of the relaxation performed in (4). This relaxation translates to diversity since it allows for sub-optimal and local minima to be generated. But an increase in entropy may not always translate to an increase in diversity, since the diversity that we are interested in is that of essentially different outputs. A generator that produces weight vectors that differ only by trivial scale transformations should not score high on diversity, even though it may have high entropy (when the scale differences are large). Similarly, the entropy may be high due to trivial logits' bias differences and not due to diversity. To deal with this problem, we update the optimistic choice (3) to contain a gauge fixing (a term used in theoretical physics), which chooses only one representative from each equivalence class of weights which are related by a scaling transformation or a logits' bias transformation. Thus, the gauge fixing breaks the symmetry that is present in the problem. The gauge fixing can be realized by requiring that  $\mathcal{G}(\theta) = 0$  for some function  $\mathcal{G}$ . This function must obey the condition that if  $\mathcal{G}(\theta) = 0$ , then  $\mathcal{G}(\theta') \neq 0$  for each  $\theta'$  that is related to  $\theta$  by a trivial symmetry transformation. The optimistic choice (3) is now transformed to:

$$p(\theta|p_{\text{data}}) = \begin{cases} \frac{1}{Z} & \text{if } \mathcal{L}(\theta|p_{\text{data}}) = \min_{\theta'} \mathcal{L}(\theta'|p_{\text{data}}) \text{ and } \mathcal{G}(\theta) = 0 \\ 0 & \text{otherwise} \end{cases} \quad (7)$$

We choose the gauge fixing term  $\mathcal{G}(\theta)$  to break the symmetries in scaling and in logits' bias. The former is broken by requiring  $\sum_k (\theta_{l,i}[k])^2 = n_{l,i}$ , where  $\theta_{l,i}[k]$  is the  $k$ 'th element of the  $i$ 'th filter of the  $l$ 'th layer, and  $n_{l,i}$  is the number of elements in the filter, including the bias term. The sum is over all elements of the filter, including the bias term. This constraint is applied to all layers  $1 \leq l \leq m-1$  where  $m$  is the number of layers, and for all filters  $i$  in the layer. This constraint breaks the scaling symmetry. It is imposed on all but the last layer, since this is the freedom we have under the scaling symmetry transformation. To see this, we can take an arbitrary network, and repeat the following process, starting with  $l=1$  and then incrementing  $l$  by 1: we scale the filters of the  $l$ 'th layer to obey the constraint, and unscale the filters of the  $l+1$  layer accordingly to keep the output unchanged. This process cannot be performed when  $l=m$ , since for the last layer there is no

---

<sup>4</sup>In this case,  $p_\varphi(\theta)$  can be written as a product of a delta function distribution and a finite distribution, where the delta serves as the restriction to the low dimensional manifold. The integration is understood to be only over this manifold, using the finite component of  $p_\varphi(\theta)$ . It can be seen from (3) that  $p(\theta|p_{\text{data}})$  never vanishes on this manifold.

next layer to do the unscaling on. We see that any network is equivalent, under the scaling transformation, to a network which satisfies this constraint. The logits' bias symmetry is broken by requiring  $\sum_i \theta_{m,i}[\text{bias}] = 0$ , where  $\theta_{m,i}[\text{bias}]$  is the bias term of the filter  $\theta_{m,i}$ . Incorporating the breaking of the symmetry with respect to the permutation transformation is also possible, for example by lexicographically sorting filters in a layer. However, we decide to ignore this symmetry, due to implementation constraints. Note that the permutations form a discrete group, and it is harder for a continuous generator to fail by generating discrete transformations.

One strategy for imposing the constraints is by turning them into quadratic terms in  $\mathcal{G}$ :

$$\mathcal{G}(\theta) = \sum_{l=1,i}^{l=m-1} \left( \sum_k (\theta_{l,i}[k])^2 - n_{l,i} \right)^2 + \left( \sum_i \theta_{m,i}[\text{bias}] \right)^2 \quad (8)$$

The relaxed form for this distribution is:

$$p(\theta|p_{\text{data}}) = \frac{\exp(-\lambda \mathcal{L}(\theta|p_{\text{data}})) \exp(-\gamma \mathcal{G}(\theta))}{Z}, \quad (9)$$

where  $\gamma > 0$  is another hyperparameter that controls the amount of relaxation of the gauge fixing. The loss function now becomes:

$$L = \lambda \mathbb{E}_{\theta \sim p_\varphi} \mathcal{L}(\theta|p_{\text{data}}) + \gamma \mathbb{E}_{\theta \sim p_\varphi} \mathcal{G}(\theta) + \mathbb{E}_{\theta \sim p_\varphi} \log p_\varphi(\theta) \quad (10)$$

The first term in  $L$  is the accuracy loss, and the other two terms combined are the diversity loss. Ignoring the regularization hyperparameters, this loss function is equivalent to the objective used in variational Bayesian inference[14], as was used in [6, 7]. Under the equivalence,  $\exp(-\mathcal{G})$  plays the role of a prior distribution for  $\theta$ , but is chosen in most works to be a diagonal Gaussian instead of a symmetry breaking term;  $-\mathcal{L}$  is the mean log-likelihood of the data given  $\theta$  under the generative model defined by the target network; and  $p_\varphi$  is an approximation to the posterior distribution of  $\theta$  given the data.

A second strategy is to impose the gauge on the hypernetwork directly, by transforming each output  $\theta$  to the required gauge. This means that the second condition in (7) will always hold, and there is no need to choose an explicit form for  $\mathcal{G}$  and to relax it. Denoting by  $S(\theta)$  a function  $\Theta \rightarrow \Theta$  that transforms every  $\theta$  to the required gauge, writing the loss function in terms of  $G$  and  $z$  gives:

$$L(\varphi|p_{\text{noise}}, p_{\text{data}}) = \mathbb{E}_{z \sim p_{\text{noise}}} [\lambda \mathcal{L}(G(z; \varphi)|p_{\text{data}}) + \log p_\varphi(S(G(z; \varphi)))] \quad (11)$$

(we do not need to include  $S$  in the  $\mathcal{L}$  term since by definition  $S$  does not alter  $\mathcal{L}$ ).

By the Gibbs relaxation, we've seen that the entropy naturally arises as a candidate to be included in the diversity term. Variational inference suggests that we take the accuracy term to be the mean of the negation of the log likelihood. In this work, we use these suggestions. However, we stress that a more general form for a loss function suitable for training a hypernetwork is (1), where the diversity term includes gauge fixing. Therefore, other measures of diversity and accuracy can be used, such as the variance, or diversity terms that are used in texture synthesis[15] and feature visualization[16]. Moreover,

in some applications we might not have the freedom to choose  $\mathcal{L}$ , as it will be given as part of the problem specification. Our formalism does not assume that there is any probabilistic interpretation of the target network’s output or of  $\mathcal{L}$ .

In this work, we use the log likelihood accuracy component for the loss function:

$$L_{\text{accuracy}}(\varphi | p_{\text{noise}}, p_{\text{data}}) = -\mathbb{E}_{z \sim p_{\text{noise}}, (x, y) \sim p_{\text{data}}} \log T(x; G(z; \varphi))_y \quad (12)$$

where for simplicity we assumed here that the data contains only deterministic distributions  $y$  (i.e.  $y$  is a one-hot encoding of the class). The subscript in  $T(x; G(z; \varphi))_y$  refers to the probability estimation for the  $y$  class given by the output of neural network  $T(\cdot; G(z; \varphi))_y$  for input  $x$ .

For the diversity component we take the last term of (11):

$$L_{\text{diversity}}(\varphi | p_{\text{noise}}) = \mathbb{E}_{z \sim p_{\text{noise}}} \log p_{\varphi}(S(G(z; \varphi))). \quad (13)$$

### 2.3 Entropy Estimation

To backpropagate through the entropy term, using minibatches of samples of  $z$ , we will need to use an estimator for differential entropy. We use the Kozachenko-Leonenko estimator[17, 18]. For a set of samples  $\theta_1, \theta_2, \dots, \theta_N$ , the estimator is:

$$\hat{H} = \psi(N) + \frac{d}{N} \sum_{i=1}^N \log(\epsilon_i), \quad (14)$$

where  $\psi$  is the digamma function,  $d$  is the dimension of the samples, which we take to be the dimension of  $z$ , and  $\epsilon_i$  is the distance from  $\theta_i$  to its nearest neighbor<sup>5</sup>. We omit terms in the definition of the estimator which are constants that do not matter for optimization<sup>6</sup>. This estimator is biased[19] but consistent in the mean square.

### 2.4 Architecture

In this section we describe the architecture for the hypernetwork  $G$ , and we assume that the target network  $T$  is convolutional where within each layer the filters have the same size. If  $G$  were a fully connected multilayer perceptron (MLP), it would scale badly as the dimension of the weights of  $T$  increases. We therefore utilize weight sharing in  $G$  by giving it a convolutional structure, see Fig. 1. The network consists of  $m + 1$  sub-networks, which we denote  $E, W_1, \dots, W_m$ , where  $m$  is the number of layers in the target network  $T$ .  $W_l$  takes as input a low dimensional vector  $c$ , which we think of as a *code*, and produces a single filter for the  $l$ ’th layer of  $T$ . We refer to the  $W_l$ ’s as *weight*

<sup>5</sup>The original estimator takes  $d$  to be the dimension of  $\theta$ . However, as explained in the previous footnote, we are interested in an estimation of the differential entropy only on the manifold defined by  $G(z)$ , stripping away the delta functions that restrict  $\theta$  to the manifold. We are using the Euclidean metric on the space  $\Theta$ , although a better estimator would use the metric induced on the lower dimensional manifold. We don’t do this due to the complications that it introduces.

<sup>6</sup>The reason that we did keep the terms  $\psi(N)$  and  $\frac{d}{N}$  is that  $N$  represents the batch size during training, but it also represents the size of the validation set during validation. If we want the entropy units to be comparable between the two, we need to keep the dependence on  $N$ , even though it does not matter for the optimization.

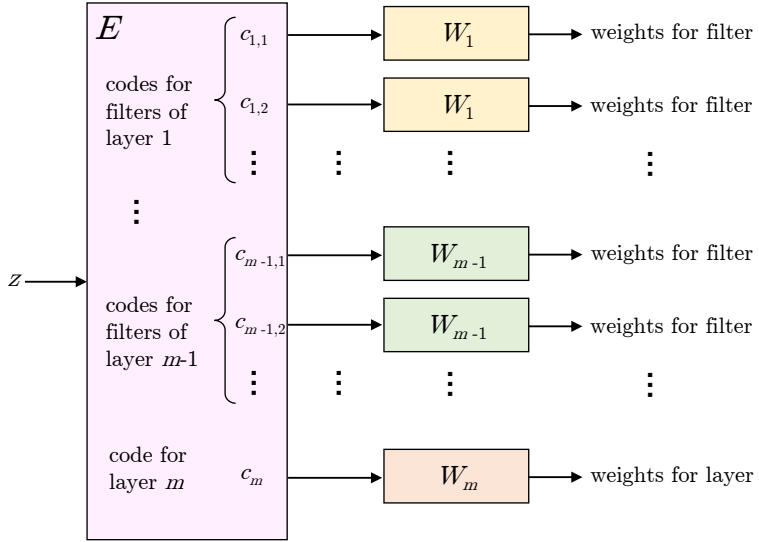


Figure 1: Architecture block diagram of the hypernetwork.  $c_{l,i}$  refers to the code for the  $i$ 'th filter in the  $l$ 'th layer.  $c_m$  is the code for the last layer.

*generators.* The block  $E$  takes the hypernetwork input  $z$ , and creates all codes for all the filters in  $T$ . We refer to  $E$  as the *extractor*, since it extracts from the latent representation  $z$  all the codes needed for producing the filters. Each code is fed into the corresponding weight generator so that weights are produced for the corresponding filter. We emphasize that the same weight generator is re-used for all filters in a certain layer of  $T$ , which results in a lot of parameter sharing.  $W_l$  can be seen as a convolutional non-linear filter with a receptive field that is a single code for the layer  $l$ . To allow a flexible use of high level features, we treat all weights in the last layer of  $T$  as one ‘‘filter’’, thus using  $W_m$  only once.

### 3 Related Work

There are many methods of using auxiliary neural networks for the task of obtaining the weights of a target network. An early example is fast weights[20], where the target network is trained together with an auxiliary memory controller(MC) network, whose goal is to drive changes in the weights of the target network. Although the overall architecture of this approach is quite similar to hypernetworks as presented here, the approach differs in two important aspects: **(a)** Fast weights are designed specifically as alternatives to recurrent networks for temporal sequence processing, and therefore the MC can never be decoupled from the target network, even after the MC has done a computation; **(b)** The input to the MC is just the input to the target network, and there is no attempt to generate diverse iid samples of the target network weights.

Under the paradigm of *learning to learn*, the works[21, 22] have trained auxiliary neural networks to act as optimizers of a target network. The optimizers apply all the updates to the target network’s weights during its training. As

opposed to the method presented here, these trained optimizers can generate weights to the target network only by receiving a long sequence of batches of training examples. On the other hand, these optimizers can generalize to various loss functions and problem instances.

In [23], the auxiliary network is used for one-shot learning: It receives as input a single training example, and produces weights for the target network. This is different from hypernetworks, where the input is a latent representation of the target network, and the generated weights are not seen as a generalization from a single training example. A related method is dynamic filter networks[24], where the auxiliary network is fed with the same input as the target network, or with a related input (such as previous frames of a video). The goal is to make the target network more adaptive to the instantaneous input or task, rather than to generate diverse versions of the target network which are on an equal footing.

It has been shown[25] that for common machine learning tasks, there is a redundancy in the raw representation of the weights of several neural network models. [8] exploits this fact to train a small neural network that generates the weights for a larger target network. This has the advantage of reduced storage size in memory, and can also be seen as a means of regularization. However, the weight generating network in [8] does not have a controllable input, and therefore it cannot be used to generate diverse random samples of weights.

Most similar to the current paper are the Bayesian hypernetworks(BHNs)[6] and multiplicative normalizing flows with Gaussian posterior(MNFGs)[7]. Both of these works formalize the problem in a Bayesian setting and use variational inference[26, 14] to get approximate samples from the posterior of the target network’s weights. A key ingredient used by both is a normalizing flow(NF)[27], which serves as a flexible invertible function approximator. A NF requires that the input size is equal to the output size, and thus requires a large hypernetwork for large target networks. To reduce the number of parameters in the hypernetwork, BHNs and MNFGs employ reparameterizations of the weights. In BHN[6], the chosen reparameterization is weight normalization[28], and the NF produces samples only of the norms of the filters. The remaining degrees of freedom are trained to be constant (non-random). MNFG[7] models the weights as a diagonal Gaussian when conditioned on the NF, with trainable means and variances. The NF acts as scaling factors on the means, one scale factor per filter (in the case of convolutional layers). The sources of randomness are thus the NF input and the per-weight Gaussian. The weights for different layers are generated independently. This limits the diversity of generated networks, since each layer needs to learn how to generate weights which give good accuracy without having any information about the other layers’ weights. In contrast, we don’t use a NF, relying instead on multilayer perceptrons (MLPs) and convolutions to create a flexible distribution. This makes it possible to use a small vector as the latent representation of primary network, while generating all of its weights, without the need to use a restrictive model (e.g Gaussian). The downside of this approach is that the MLPs are not invertible, which might cause the output manifold to have a lower dimension than the input, and which makes it necessary to use an approximation for the entropy of the output.

There are other Bayesian approaches for weight generation, which do not use a neural network as a generator. Markov Chain Monte Carlo[29, 30] use a Markov chain in the weight space with equilibrium distribution that equals the

required posterior. In [31, 32], the posterior is approximated as a diagonal Gaussian with trainable means and variances, and the variational inference[26, 14] objective is used. Another variational inference method is [33], which approximates the posterior of the weights as proportional to Bernoulli variables, which is equivalent to the dropout regularization technique[34].

## 4 Experiments

To run experiments, we implemented a hypernetwork in TensorFlow[35]. All code used to run these experiments can be found online<sup>7</sup>. Please refer to the code to see a full specification of hyperparameter values and implementation details.

### 4.1 Toy Problem

We start with a toy problem which is easy to visualize. Instead of generating weights for a neural network, we generate a two dimensional vector. The goal is that the generated vectors have high values on a specified Gaussian mixture, and also obtain high diversity. We take the input  $z$  to the hypernetwork to have dimension 1, to demonstrate the case where the hypernetworks output manifold has a lower dimensionality than the space of all weight configurations. This problem does not have symmetries, so we do not include the term  $S$  in the loss. Instead, we use a conventional  $\ell_2$  regularization loss. The hypernetwork is taken as a MLP whose hidden layers have sizes 30, 10 and 10. The final distribution learned by the hypernetwork can be seen in Fig. 2. We see that the one dimensional distribution is supported on a path which passes through all peaks of the Gaussian mixture. Inevitably, the path must pass through regions with low values of the Gaussian mixture. However, in these regions the density is lower.

### 4.2 MNIST

Here, we take the target network architecture  $T$  to be a simple convolutional network for classifying images of the MNIST data set[36]. The data set members are  $28 \times 28$  grayscale images of handwritten digits, with the label set being  $\{0, \dots, 9\}$ . The training set has 55000 images, and the test set has 10000 images. The target network architecture is displayed in Table 1. It is comprised of two convolutional layers, with 32 and 16 filters respectively, followed by two fully connected layers, with 8 and 10 filters (neurons) respectively. The output is a 10-dimensional vector of probabilities for each class. The total number of weights in the network is 20018. This network can easily be trained to achieve an accuracy of over 99% on the test set.

The specifications of the architecture for the hypernetwork are given in Table 2. We choose the input  $z$  to the network to be a 300 dimensional vector, drawn from a uniform distribution over  $[-1, 1]^{300}$ . The code sizes for the weight generators are chosen to be 15 for all four layers. The extractor and the weight generators are all MLPs with leaky-ReLU[13] activations. Batch normalization[39] is used in all layers besides the output layers of each sub-network. We do not use

---

<sup>7</sup><https://github.com/sliorde/generating-neural-networks-with-neural-networks>

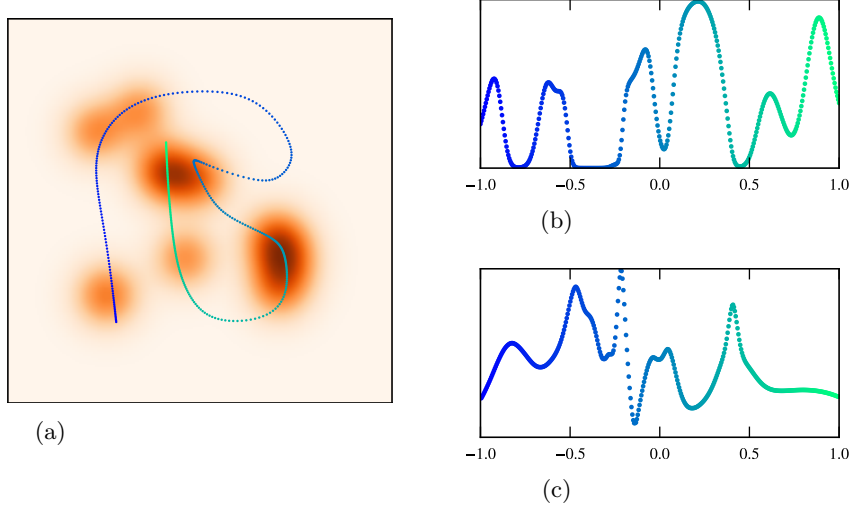


Figure 2: The hypernetwork on a toy example in two dimensions. **(a)** The background image has the values of the Gaussian mixture, in shades of orange. The one dimensional structure (which is composed of points) is the distribution learned by the hypernetwork. This distribution is the image under the hypernetwork of the set of 400 uniformly spaced points in the range  $[-1, 1]$ . The points were colored so that they can be easily matched with the other two graphs in this figure. **(b)** The values of the Gaussian mixture along the path **(c)** The distance of each point in the path to its nearest neighbor. This graph demonstrates that the density of points is lower in regions of lower values of the Gaussian mixture.

bias parameters in the hypernetwork, since our empirical evidence suggests (albeit inconclusively) that this helps for diversity. The total number of parameters in  $G$  is 633640.

We trained the hypernetwork using the Adam optimizer[40]. The gradients of the loss were estimated using minibatches of 32 samples of  $z$ , and 32 images per sample of  $z$  (we use different images for each noise sample). We found that this relatively large batch size is a good operating point in terms of the tradeoff between estimator variance and learning rate. We trained on a total of 13000 minibatches, and this took about 30 minutes on a single NVIDIA Tesla K80 GPU.

We compare our results to MNFG[7]. We used code that is available online<sup>8</sup>, and modified it so that it generates the same target networks as our hypernetwork.

#### 4.2.1 Accuracy

The accuracy of generated networks depends on the hyperparameter  $\lambda$ . Figs. 3a,3b display histograms of the accuracies of the generated weights, for  $\lambda = 10^5$  and  $\lambda = 10^3$  respectively. We also show the corresponding histogram for MNFG in Fig. 3c. From now on, we will use  $\lambda = 10^3$ , which yields lower accuracies, but

<sup>8</sup>[https://github.com/MLab-Amsterdam/MNF\\_VBNN](https://github.com/MLab-Amsterdam/MNF_VBNN)

layer name	layer components	number of weights	output size
input image			$28 \times 28 \times 1$
layer1	convolution: $5 \times 5$ , stride: $1 \times 1$ , padding: ‘SAME’, number of filters: 32	832	
	activation: ReLU		
	max pool: $2 \times 2$ , stride: $2 \times 2$ , padding: ‘SAME’		$14 \times 14 \times 32$
layer2	convolution: $5 \times 5$ , stride: $1 \times 1$ , padding: ‘SAME’, number of filters: 16	12816	
	activation: ReLU		
	max pool: $2 \times 2$ , stride: $2 \times 2$ , padding: ‘SAME’		$7 \times 7 \times 16$
layer3	fully-connected, number of filters: 8	6280	
	activation: ReLU		8
layer4	fully-connected, number of filters: 10	90	
	softmax		10

Table 1: The target network architecture. Note that all layers also have bias parameters. See [37, 38] for definitions of the various terms.

sub-network	layer structure	number of parameters
$E$	$300 \rightarrow 300 \rightarrow 300 \rightarrow 855 = 15 \cdot (32 + 16 + 8 + 1)$	436500
$W_1$	$15 \rightarrow 40 \rightarrow 40 \rightarrow 26 = 5 \cdot 5 + 1$	3240
$W_2$	$15 \rightarrow 100 \rightarrow 100 \rightarrow 801 = 5 \cdot 5 \cdot 32 + 1$	91600
$W_3$	$15 \rightarrow 100 \rightarrow 100 \rightarrow 785 = ((28^2)/(4^2)) \cdot 16 + 1$	90000
$W_4$	$15 \rightarrow 60 \rightarrow 60 \rightarrow 90 = (8 + 1) \cdot 10$	9900

Table 2: The layer structures for each of the fully-connected sub-networks of the hypernetwork. The layer structures are in the format (input size)  $\rightarrow$  (first layer size)  $\rightarrow$  (second layer size)  $\rightarrow$  (output size). The sub-networks do not include bias terms. The number of parameters shown here does not include the batch normalization parameters.

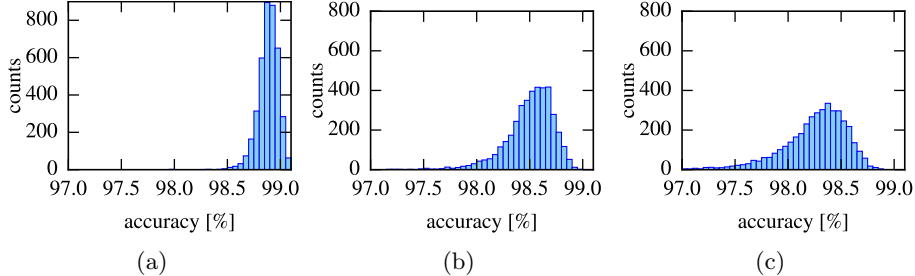


Figure 3: Histograms of ac curacies of generated networks. (a) Our hypernetwork,  $\lambda = 10^5$  (b) Our hypernetwork,  $\lambda = 10^3$  (c) MNFG

they are more comparable to the results of MNFG and therefore form a good basis for comparison.

#### 4.2.2 Diversity

We explore the diversity in a few different ways. The histograms in Fig. 3 gives an initial indication of diversity by showing that there is variance in the generated networks' accuracies.

**Visual Inspection.** In Figs. 7-10 we show images of different samples the produced filters. By visual inspection we see that there are different forms that these filters can take. However, it is noticeable that there are some repeating patterns in the generated filters. For comparison, we show corresponding images for MNFG in Figs. 11-13, where we gauged the MNFG filters just as our own. By visual inspection we see that MNFG yields high diversity for most filters (e.g. Fig. 11), but very low diversity for others (Fig. 12), mainly in the first layer. We see this phenomena also in our generated filters only to a lesser extent. We hypothesize that a possible mode of failure for hypernetworks is that it focuses much of its diversity in specific filters, while making sure that these filters get very small weights in the next layer, thereby effectively canceling these filters. Future work should consider this mode of failure in the diversity term of the loss function.

**Scatter.** One may wonder whether our method of weight generation is equivalent to trivially sampling from  $\mathcal{N}(\theta_0, \Sigma)$ , for some optimal weight vector  $\theta_0$  and constant  $\Sigma$ . To see that this is not the case, we view the scattering of the weight vectors in the principal components given by the principle component analysis (PCA). This is shown in Figs. 14 - 21. We see that the hypernetwork learned to generate a distribution of weights on a non-trivial manifold, with prominent one dimensional structures. In Figs. 22 - 26 we display the same kind of scatter graphs for MNFG.

**Paths in Weight Space.** Another way to probe the diversity is by evaluating the accuracy along paths in the weight space  $\Theta$ . For two given input vectors  $z_1$  and  $z_2$ , we define two paths: The direct path  $\{G(z_1)t + G(z_2)(1-t) \mid t \in [0, 1]\}$ , and the interpolated path  $\{G(z_1t + z_2(1-t)) \mid t \in [0, 1]\}$ . These two paths coincide in their endpoints. We expect high accuracy along the interpolated path. Whether the direct path has high accuracy depends on the nature of the generated manifold. If the diversity is achieved only via random noise around a specific weight vector (such as in the trivial case mentioned in the last para-

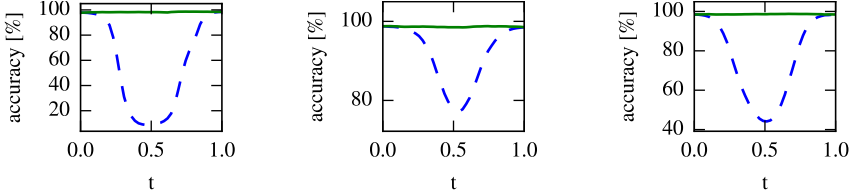


Figure 4: Accuracies along paths, with end points  $z_1, z_2$  sampled at random. Each graph corresponds to a different sampled pair of endpoints. The dashed lines are the direct paths, and the solid lines are the interpolated paths.

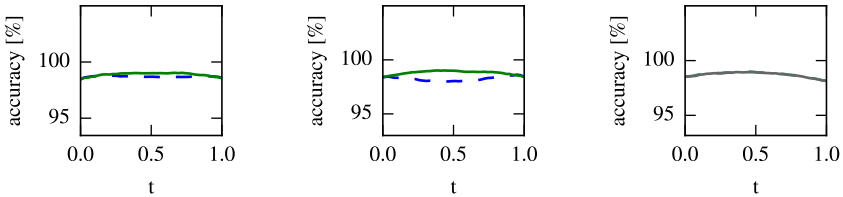


Figure 5: Accuracies along paths, with end points  $z_1, z_2$  sampled at random, for MNFG. Each graph corresponds to a different sampled pair of endpoints. The dashed lines are the direct paths, and the solid lines are the interpolated paths.

graph), the direct path would have high accuracy. In Fig. 4 we see that this is not the case. The analogous graph for MNFG, displayed in Fig. 5, shows that for MNFG the direct path does give high accuracy. A possible explanation for this is that MNFG generates scale factors for the weights, and therefore the generated manifold is approximately linear.

**Ensembles.** As a last measure of diversity, we compare the accuracy of the generated networks with the accuracy of ensembles of generated networks. If the generated classifiers are sufficiently different, then combining them should yield a classifier with reduced variance[41], and therefore lower error. We created 20 ensembles, each of size 200, and we take their majority vote as a classification rule. The result is that the average accuracy of the ensembles on the test set was 99.14%, which is higher than typical results that we see in the histogram in Fig. 3. For MNFG, the same experiment gives an average ensemble accuracy of 99.28%.

#### 4.2.3 Adversarial Examples

Adversarial examples [42, 43] are inputs to classification networks which are deliberately crafted by an adversary to cause the network to miss-classify them. As a final application of hypernetworks, we show that using ensembles of generated networks can help reduce the sensitivity to adversarial examples. The experiment was conducted by following these steps: **1)** Use the hypernetwork to generate a weight vector  $\theta$ . **2)** Sample a pair  $(x, y)$  of image and label from the test set (make sure to choose a pair which is correctly classified by the classifier with weights  $\theta$ ). **3)** Randomly pick a new label  $y' \neq y$  to be the target class of the adversarial example. **4)** Use the fast gradient method[43] to generate

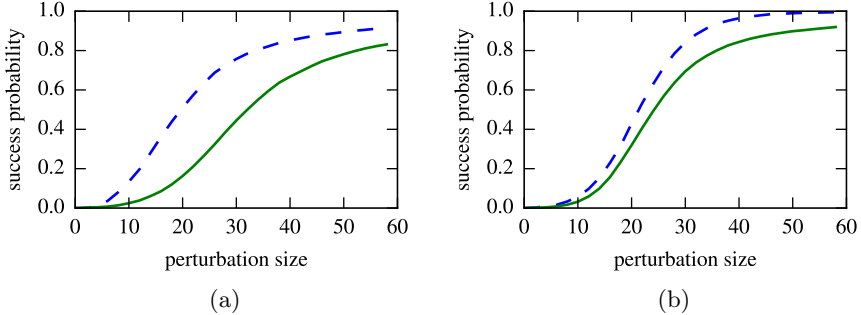


Figure 6: The success probability of adversarial examples created with the fast gradient method with a given perturbation size, against an ensemble of 100 generated networks. The dashed lines are the single classifier, and the solid lines are ensembles. (a) our hypernetwork. (b) MNFG.

adversarial examples. Do this for perturbation sizes  $\epsilon$  in the range 0 to 0.24, where these numbers are fractions of the full dynamic range of an image (i.e. 1 corresponds to 8 bits of grayscale). **5)** Test which values of  $\epsilon$  yield adversarial examples that fool the classifier with weights  $\theta$ . **6)** Use the hypernetwork to generate an ensemble of 100 classifiers, and test for which values  $\epsilon$  the adversarial examples that were generated in step 4 fool the ensemble. We repeat this experiment over all images in the test set. The results are shown in Fig. 6, together with results for MNFG. We see that the probability of success for an adversarial attack is reduced when using ensembles.

hyperbetwork

## 5 Discussion

In this work we've shown how a hypernetwork can be trained to generate accurate and diverse weight vectors. This work should be taken as a proof of concept that requires further development, and a more extensive search over hyperparameter space. There are many directions of further inquiry that we haven't touched upon in this work, for example: Is there a certain gauge which yields better training? How should we divide our units of compute between the extractor and the weight generators? What are the performances of other metrics for diversity, besides entropy? What are good methods for initializing parameters for the hypernetwork? In answering this last question, one should notice that popular methods (for example, [44, 45]), use the  $\text{fan}_{\text{in}}$  and  $\text{fan}_{\text{out}}$  of a unit, but in the case of a weight generator sub-network in our architecture, we may want to take into account also the  $\text{fan}_{\text{in}}$  and  $\text{fan}_{\text{out}}$  of the generated filter.

Another research direction to pursue is the question of whether the diversity term is necessary at all. In experiments which we haven't described in section 4, we seem to see that when using large initial values for the parameters, the generated manifold spans a region large enough to be in the proximity of multiple local minima of the accuracy loss. When optimizing only over the accuracy (and not the diversity), the manifold "clumps" around these local minimizers. If they are numerous enough, then we may get diverse results without needing to explicitly compromise accuracy in the loss function.

It is critical to be able to find architectures for hypernetworks which scale better with the size of the target network. Ideally, hypernetworks will have fewer parameters than their target networks, and therefore could be used as a compressed version of the target network.

We've seen already that hypernetworks can be used to form ensembles. These can be used to obtain confidence intervals on classification results, and to reduce sensitivity to adversarial perturbations. We would like to mention some additional, speculative, applications of hypernetworks. The first is copyright infringement detection: If a company distributes a product which contains a neural network, then using hypernetworks, each specific product instance can have a unique weight vector. Thus, the network can act as a "signature". We also speculate whether a network generated with a hypernetwork might have good differential privacy properties[46], which means that it is hard to extract sensitive training data given only the target network. The inspiration to this speculation comes from other works[47] which achieve differential privacy by inserting a buffer between the sensitive training set and the target classification network, in the form of an ensemble of "teacher" classification networks, which distill the information of the sensitive data and are used for training the target network. In our work, the hypernetwork may also be seen as such a buffer.

As a last note, we would like to suggest that hypernetworks can be used as a tool to probe the "space" of optimal and sub-optimal neural networks, thus allowing us to thicken our theoretical understanding of the subject.

## References

- [1] D. P. Kingma and M. Welling, "Auto-encoding variational bayes," *arXiv preprint arXiv:1312.6114*, 2013.
- [2] I. Goodfellow, J. Pouget-Abadie, M. Mirza, B. Xu, D. Warde-Farley, S. Ozair, A. Courville, and Y. Bengio, "Generative adversarial nets," in *Advances in Neural Information Processing Systems 27* (Z. Ghahramani, M. Welling, C. Cortes, N. D. Lawrence, and K. Q. Weinberger, eds.), pp. 2672–2680, Curran Associates, Inc., 2014.
- [3] C. Vondrick, H. Pirsiavash, and A. Torralba, "Generating videos with scene dynamics," in *Advances In Neural Information Processing Systems*, pp. 613–621, 2016.
- [4] S. R. Bowman, L. Vilnis, O. Vinyals, A. M. Dai, R. Jozefowicz, and S. Bengio, "Generating sentences from a continuous space," *arXiv preprint arXiv:1511.06349*, 2015.
- [5] M. Benhenda, "Chemgan challenge for drug discovery: can ai reproduce natural chemical diversity?," *arXiv preprint arXiv:1708.08227*, 2017.
- [6] D. Krueger, C.-W. Huang, R. Islam, R. Turner, A. Lacoste, and A. Courville, "Bayesian hypernetworks," *arXiv preprint arXiv:1710.04759*, 2017.
- [7] C. Louizos and M. Welling, "Multiplicative normalizing flows for variational bayesian neural networks," *arXiv preprint arXiv:1703.01961*, 2017.

- [8] D. Ha, A. Dai, and Q. V. Le, “Hypernetworks,” *arXiv preprint arXiv:1609.09106*, 2016.
- [9] A. Choromanska, M. Henaff, M. Mathieu, G. B. Arous, and Y. LeCun, “The loss surfaces of multilayer networks,” in *Artificial Intelligence and Statistics*, pp. 192–204, 2015.
- [10] Y. N. Dauphin, R. Pascanu, C. Gulcehre, K. Cho, S. Ganguli, and Y. Bengio, “Identifying and attacking the saddle point problem in high-dimensional non-convex optimization,” in *Advances in Neural Information Processing Systems 27* (Z. Ghahramani, M. Welling, C. Cortes, N. D. Lawrence, and K. Q. Weinberger, eds.), pp. 2933–2941, Curran Associates, Inc., 2014.
- [11] K. Jarrett, K. Kavukcuoglu, Y. LeCun, *et al.*, “What is the best multi-stage architecture for object recognition?,” in *Computer Vision, 2009 IEEE 12th International Conference on*, pp. 2146–2153, IEEE, 2009.
- [12] X. Glorot, A. Bordes, and Y. Bengio, “Deep sparse rectifier neural networks,” in *Proceedings of the Fourteenth International Conference on Artificial Intelligence and Statistics*, pp. 315–323, 2011.
- [13] A. L. Maas, A. Y. Hannun, and A. Y. Ng, “Rectifier nonlinearities improve neural network acoustic models,” in *Proc. ICML*, vol. 30, 2013.
- [14] D. P. Kingma, *Variational inference & deep learning: A new synthesis*. PhD thesis, University of Amsterdam, 2017.
- [15] Y. Li, C. Fang, J. Yang, Z. Wang, X. Lu, and M.-H. Yang, “Diversified texture synthesis with feed-forward networks,” *arXiv preprint arXiv:1703.01664*, 2017.
- [16] C. Olah, A. Mordvintsev, and L. Schubert, “Feature visualization,” *Distill*, 2017. <https://distill.pub/2017/feature-visualization>.
- [17] L. Kozachenko and N. N. Leonenko, “Sample estimate of the entropy of a random vector,” *Problemy Peredachi Informatsii*, vol. 23, no. 2, pp. 9–16, 1987.
- [18] A. Kraskov, H. Stögbauer, and P. Grassberger, “Estimating mutual information,” *Physical review E*, vol. 69, no. 6, p. 066138, 2004.
- [19] A. Charzyńska and A. Gambin, “Improvement of the k-nn entropy estimator with applications in systems biology,” *Entropy*, vol. 18, no. 1, p. 13, 2015.
- [20] J. Schmidhuber, “Learning to control fast-weight memories: An alternative to dynamic recurrent networks,” *Learning*, vol. 4, no. 1, 2008.
- [21] M. Andrychowicz, M. Denil, S. Gomez, M. W. Hoffman, D. Pfau, T. Schaul, and N. de Freitas, “Learning to learn by gradient descent by gradient descent,” in *Advances in Neural Information Processing Systems*, pp. 3981–3989, 2016.

- [22] K. Li and J. Malik, “Learning to optimize,” *arXiv preprint arXiv:1606.01885*, 2016.
- [23] L. Bertinetto, J. F. Henriques, J. Valmadre, P. Torr, and A. Vedaldi, “Learning feed-forward one-shot learners,” in *Advances in Neural Information Processing Systems*, pp. 523–531, 2016.
- [24] B. De Brabandere, X. Jia, T. Tuytelaars, and L. Van Gool, “Dynamic filter networks,” in *Neural Information Processing Systems (NIPS)*, 2016.
- [25] M. Denil, B. Shakibi, L. Dinh, M. A. Ranzato, and N. de Freitas, “Predicting parameters in deep learning,” in *Advances in Neural Information Processing Systems 26* (C. J. C. Burges, L. Bottou, M. Welling, Z. Ghahramani, and K. Q. Weinberger, eds.), pp. 2148–2156, Curran Associates, Inc., 2013.
- [26] G. E. Hinton and D. Van Camp, “Keeping the neural networks simple by minimizing the description length of the weights,” in *Proceedings of the sixth annual conference on Computational learning theory*, pp. 5–13, ACM, 1993.
- [27] D. J. Rezende and S. Mohamed, “Variational inference with normalizing flows,” *arXiv preprint arXiv:1505.05770*, 2015.
- [28] T. Salimans and D. P. Kingma, “Weight normalization: A simple reparameterization to accelerate training of deep neural networks,” in *Advances in Neural Information Processing Systems 29* (D. D. Lee, M. Sugiyama, U. V. Luxburg, I. Guyon, and R. Garnett, eds.), pp. 901–909, Curran Associates, Inc., 2016.
- [29] R. M. Neal, *Bayesian learning for neural networks*. PhD thesis, University of Toronto, 1995.
- [30] M. Welling and Y. W. Teh, “Bayesian learning via stochastic gradient langevin dynamics,” in *Proceedings of the 28th International Conference on Machine Learning (ICML-11)*, pp. 681–688, 2011.
- [31] A. Graves, “Practical variational inference for neural networks,” in *Advances in Neural Information Processing Systems*, pp. 2348–2356, 2011.
- [32] C. Blundell, J. Cornebise, K. Kavukcuoglu, and D. Wierstra, “Weight uncertainty in neural network,” in *International Conference on Machine Learning*, pp. 1613–1622, 2015.
- [33] Y. Gal and Z. Ghahramani, “Dropout as a bayesian approximation: Representing model uncertainty in deep learning,” in *international conference on machine learning*, pp. 1050–1059, 2016.
- [34] N. Srivastava, G. E. Hinton, A. Krizhevsky, I. Sutskever, and R. Salakhutdinov, “Dropout: a simple way to prevent neural networks from overfitting,” *Journal of machine learning research*, vol. 15, no. 1, pp. 1929–1958, 2014.

- [35] M. Abadi, A. Agarwal, P. Barham, E. Brevdo, Z. Chen, C. Citro, G. S. Corrado, A. Davis, J. Dean, M. Devin, *et al.*, “Tensorflow: Large-scale machine learning on heterogeneous distributed systems,” *arXiv preprint arXiv:1603.04467*, 2016.
- [36] Y. LeCun, L. Bottou, Y. Bengio, and P. Haffner, “Gradient-based learning applied to document recognition,” *Proceedings of the IEEE*, vol. 86, no. 11, pp. 2278–2324, 1998.
- [37] A. Krizhevsky, I. Sutskever, and G. E. Hinton, “Imagenet classification with deep convolutional neural networks,” in *Advances in neural information processing systems*, pp. 1097–1105, 2012.
- [38] K. Simonyan and A. Zisserman, “Very deep convolutional networks for large-scale image recognition,” *arXiv preprint arXiv:1409.1556*, 2014.
- [39] S. Ioffe and C. Szegedy, “Batch normalization: Accelerating deep network training by reducing internal covariate shift,” in *International Conference on Machine Learning*, pp. 448–456, 2015.
- [40] D. Kingma and J. Ba, “Adam: A method for stochastic optimization,” *arXiv preprint arXiv:1412.6980*, 2014.
- [41] J. Friedman, T. Hastie, and R. Tibshirani, *The elements of statistical learning*, vol. 1. Springer series in statistics New York, 2001.
- [42] C. Szegedy, W. Zaremba, I. Sutskever, J. Bruna, D. Erhan, I. Goodfellow, and R. Fergus, “Intriguing properties of neural networks,” *arXiv preprint arXiv:1312.6199*, 2013.
- [43] I. J. Goodfellow, J. Shlens, and C. Szegedy, “Explaining and harnessing adversarial examples,” *arXiv preprint arXiv:1412.6572*, 2014.
- [44] X. Glorot and Y. Bengio, “Understanding the difficulty of training deep feedforward neural networks,” in *Proceedings of the Thirteenth International Conference on Artificial Intelligence and Statistics*, pp. 249–256, 2010.
- [45] K. He, X. Zhang, S. Ren, and J. Sun, “Delving deep into rectifiers: Surpassing human-level performance on imagenet classification,” in *Proceedings of the IEEE international conference on computer vision*, pp. 1026–1034, 2015.
- [46] C. Dwork, “A firm foundation for private data analysis,” *Communications of the ACM*, vol. 54, no. 1, pp. 86–95, 2011.
- [47] N. Papernot, M. Abadi, Ú. Erlingsson, I. Goodfellow, and K. Talwar, “Semi-supervised knowledge transfer for deep learning from private training data,” *arXiv preprint arXiv:1610.05755*, 2016.

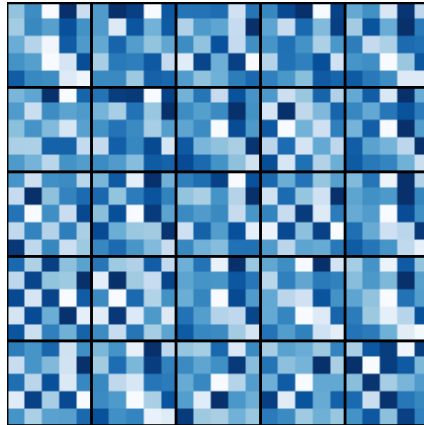


Figure 7: The large squares show different samples for one specific first layer filter of the target network.

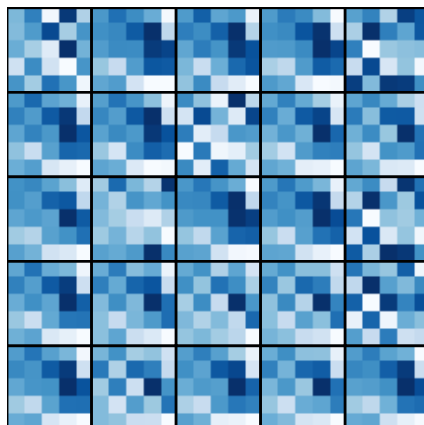


Figure 8: The large squares show different samples for one specific first layer filter of the target network.

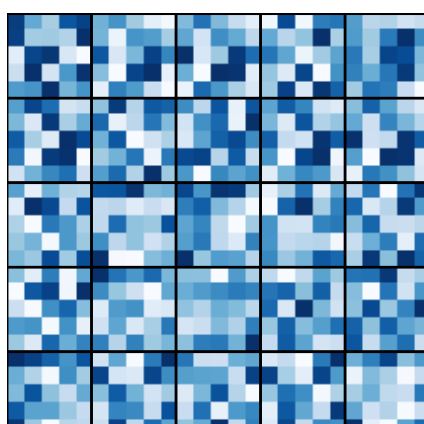


Figure 9: The large squares show different samples for one channel of a specific second layer filter of the target network.

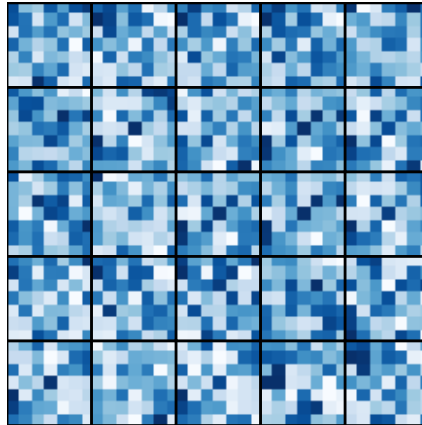


Figure 10: The large squares show different samples for one channel of a specific third layer fully-connected neuron of the target network.

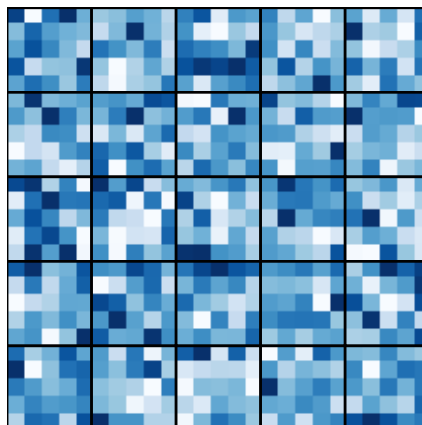


Figure 11: The large squares show different samples for one specific first layer filter of the target network, **for MNFG**.

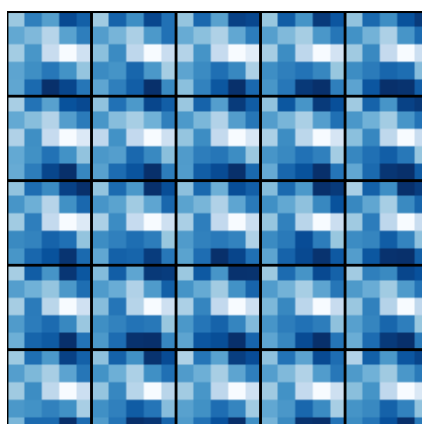


Figure 12: The large squares show different samples for one specific first layer filter of the target network, **for MNFG**.

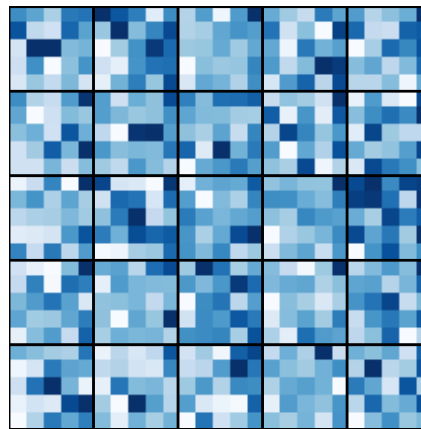


Figure 13: The large squares show different samples for one channel of a specific second layer filter of the target network, **for MNFG**.

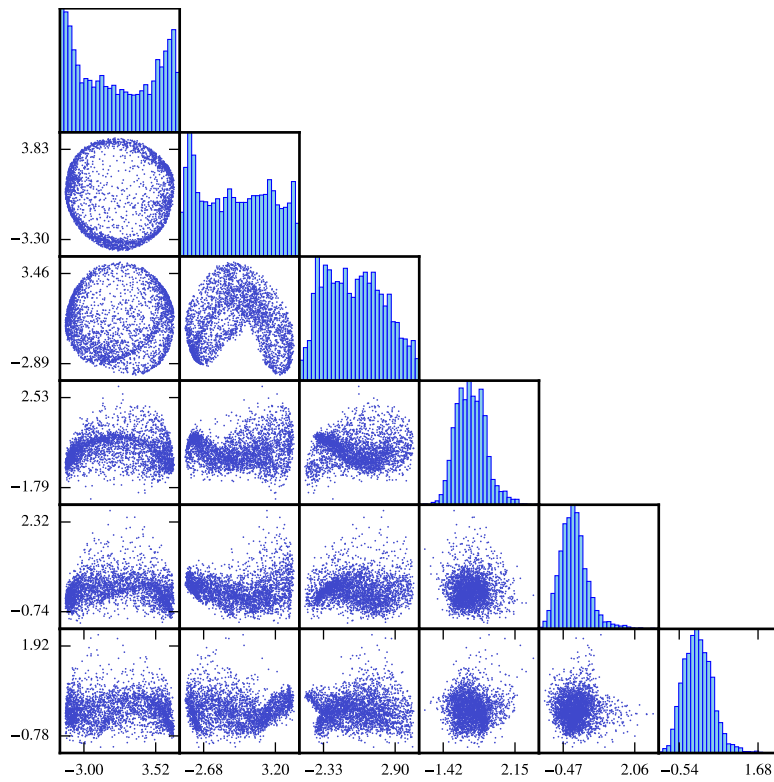


Figure 14: Scatter plots of the generated weights for a specific first layer filter, in PCA space. The  $(i, j)$  scatter plot has principal component  $i$  against principal component  $j$ . The diagonal plots are histograms.

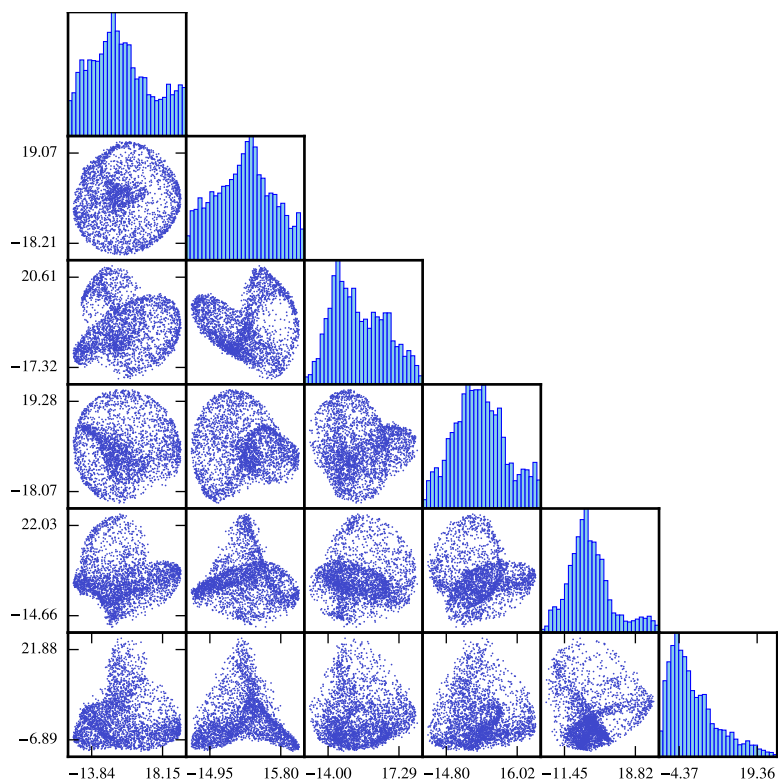


Figure 15: Scatter plots of the generated weights for a specific second layer filter, in PCA space. The  $(i, j)$  scatter plot has principal component  $i$  against principal component  $j$ . The diagonal plots are histograms.

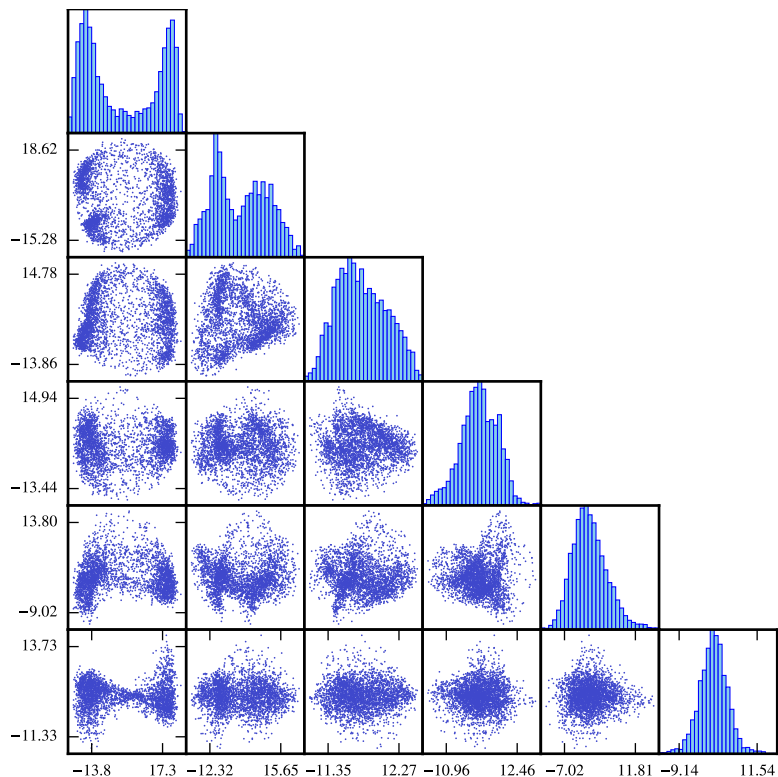


Figure 16: Scatter plots of the generated weights for a specific third layer neuron, in PCA space. The  $(i, j)$  scatter plot has principal component  $i$  against principal component  $j$ . The diagonal plots are histograms.

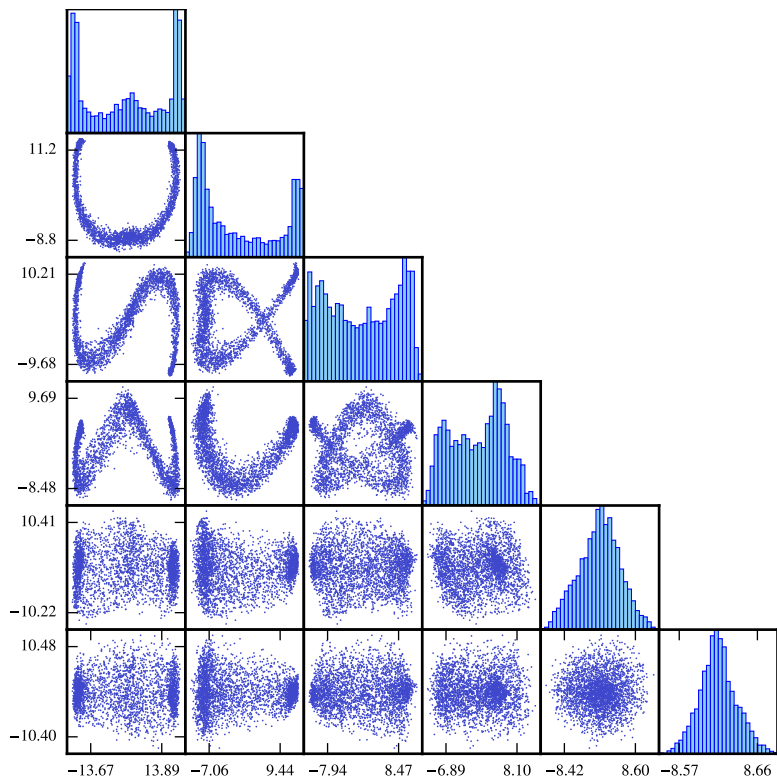


Figure 17: Scatter plots of the generated weights for the entire first layer, in PCA space. The  $(i, j)$  scatter plot has principal component  $i$  against principal component  $j$ . The diagonal plots are histograms.

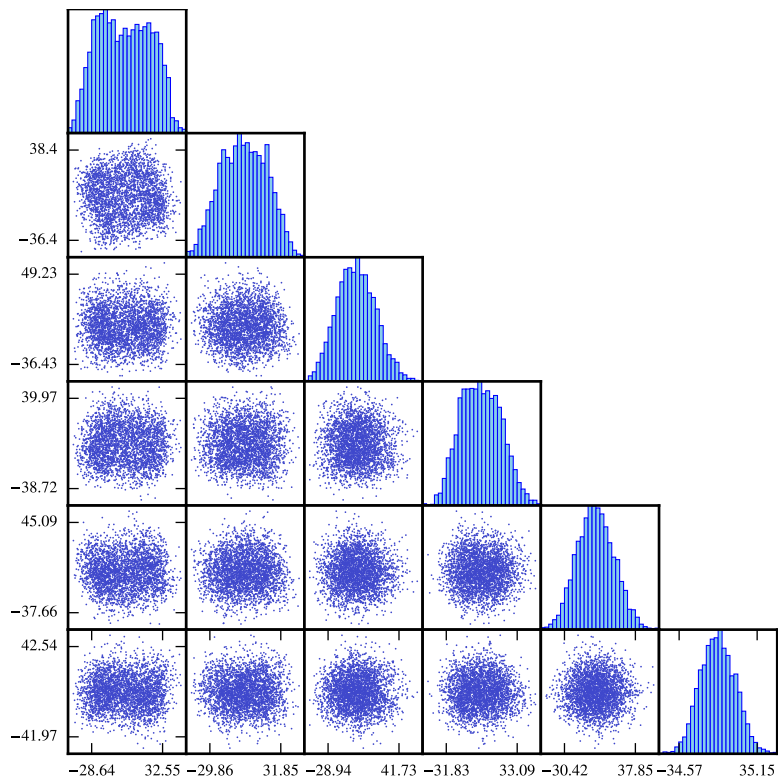


Figure 18: Scatter plots of the generated weights for the entire second layer, in PCA space. The  $(i, j)$  scatter plot has principal component  $i$  against principal component  $j$ . The diagonal plots are histograms.

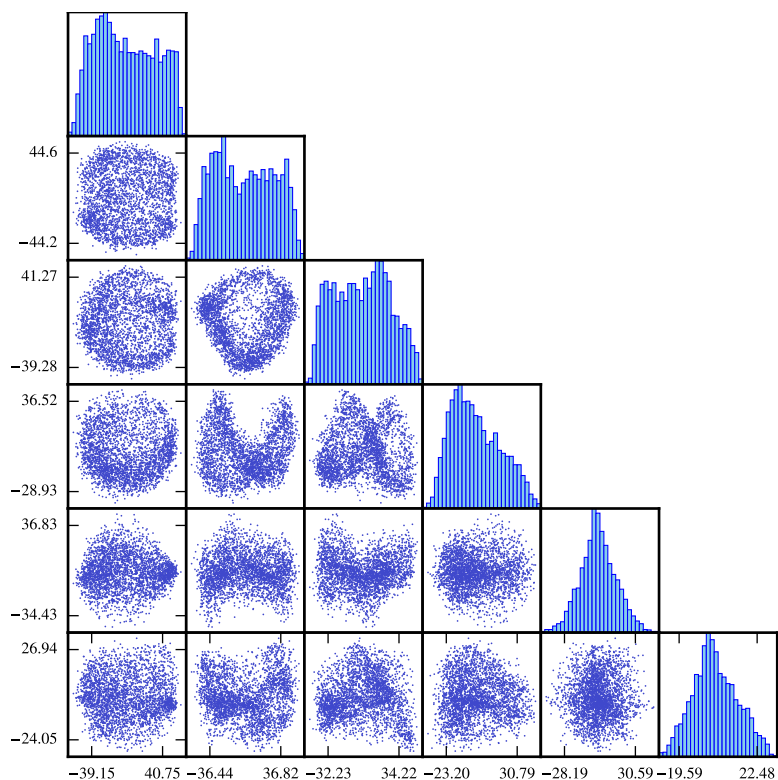


Figure 19: Scatter plots of the generated weights for the entire third layer, in PCA space. The  $(i, j)$  scatter plot has principal component  $i$  against principal component  $j$ . The diagonal plots are histograms.

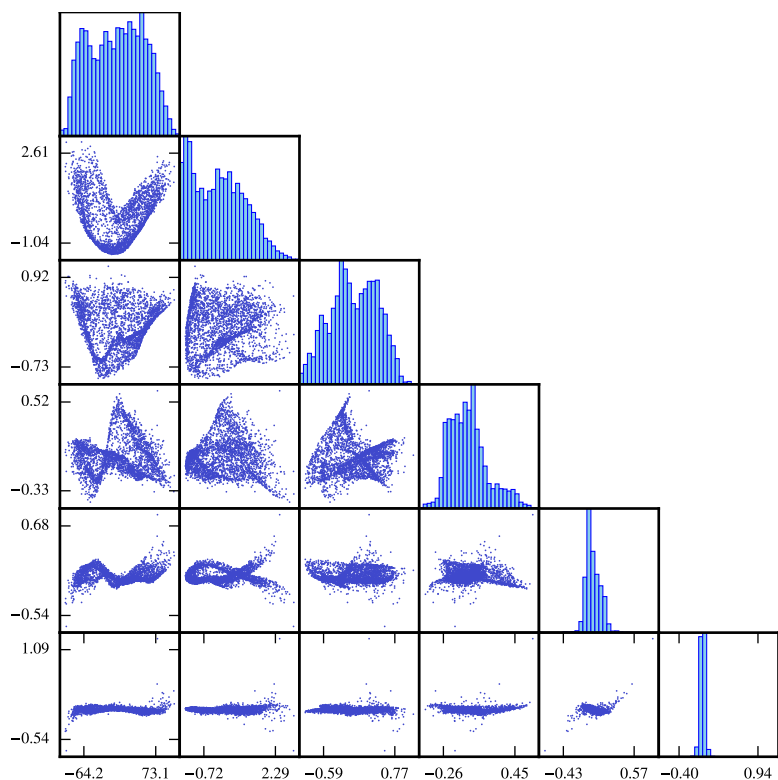


Figure 20: Scatter plots of the generated weights for the entire fourth layer, in PCA space. The  $(i, j)$  scatter plot has principal component  $i$  against principal component  $j$ . The diagonal plots are histograms.

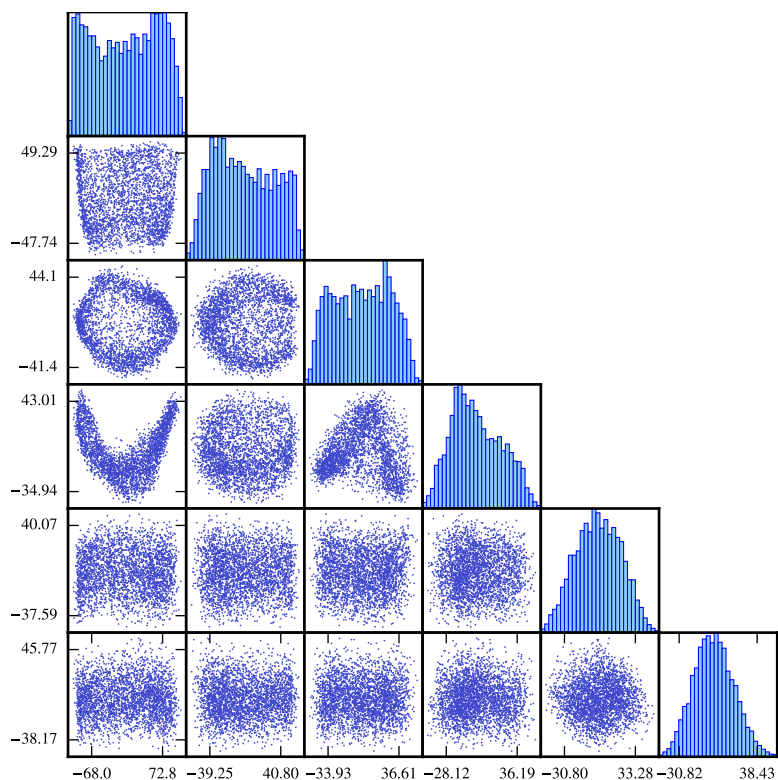


Figure 21: Scatter plots of the generated weights for the entire target network, in PCA space. The  $(i, j)$  scatter plot has principal component  $i$  against principal component  $j$ . The diagonal plots are histograms.

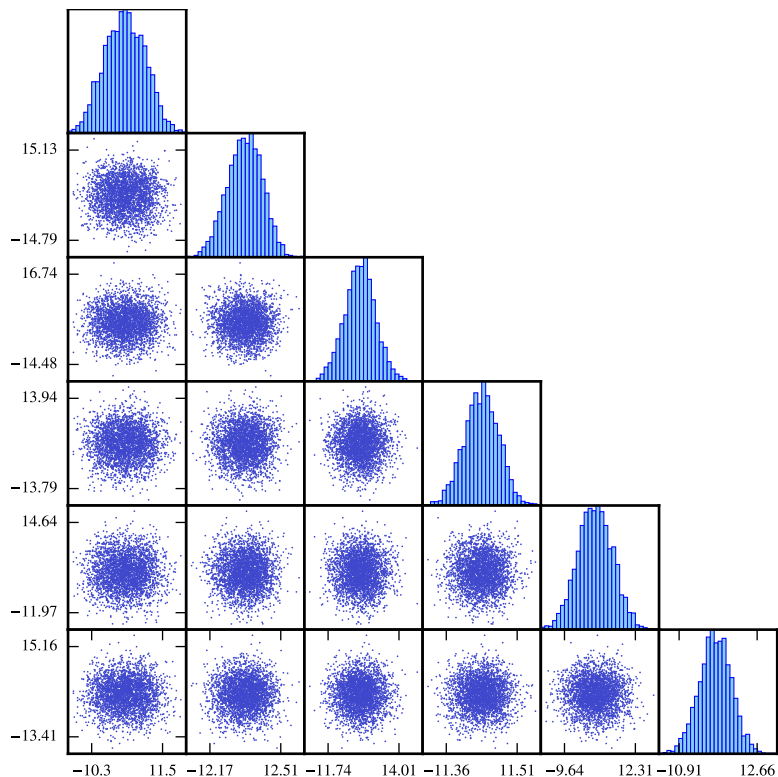


Figure 22: Scatter plots of the generated weights for the entire first layer, in PCA space, **for MNFG**. The  $(i, j)$  scatter plot has principal component  $i$  against principal component  $j$ . The diagonal plots are histograms.

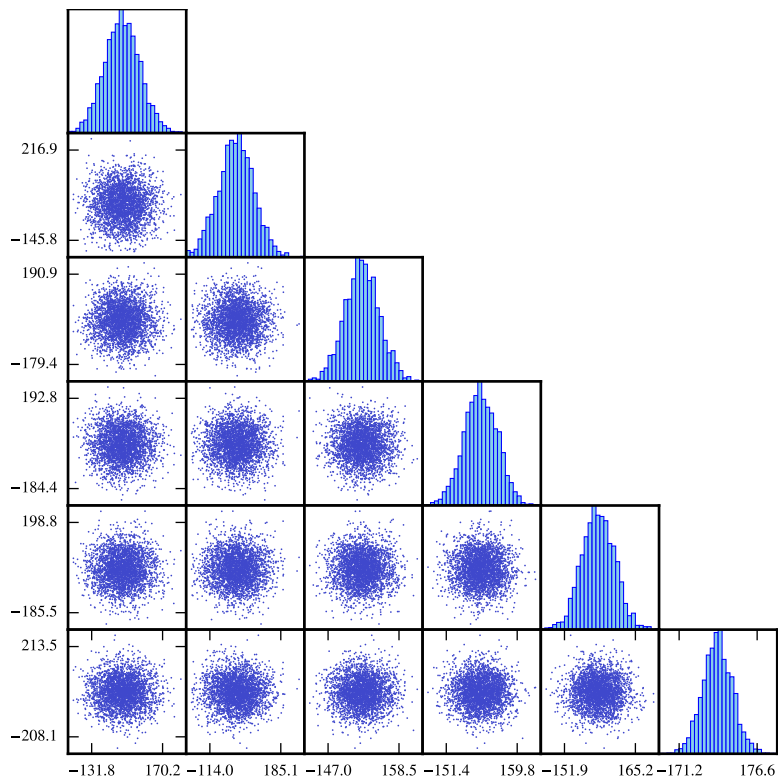


Figure 23: Scatter plots of the generated weights for the entire second layer, in PCA space, **for MNFG**. The  $(i, j)$  scatter plot has principal component  $i$  against principal component  $j$ . The diagonal plots are histograms.

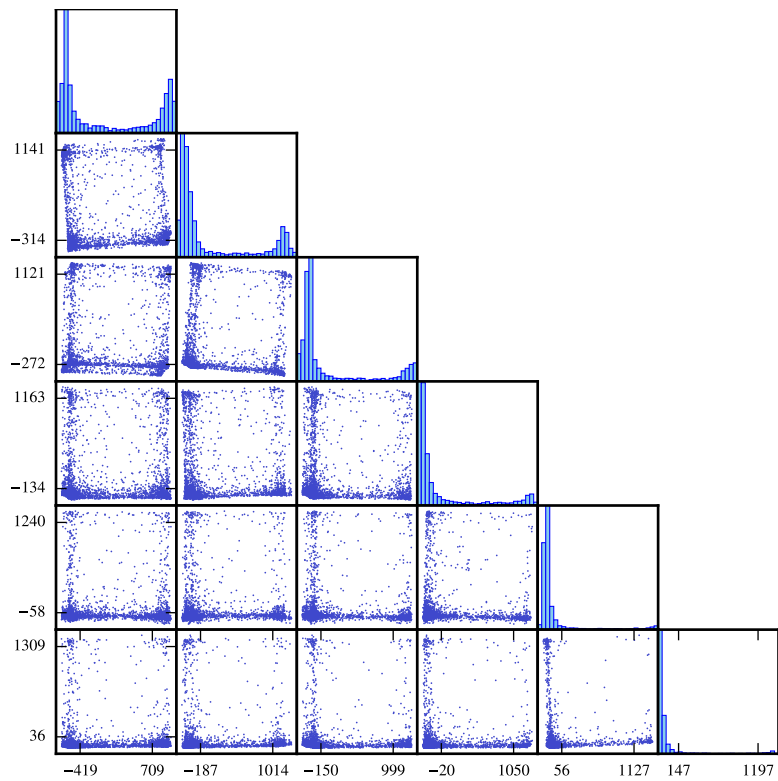


Figure 24: Scatter plots of the generated weights for the entire third layer, in PCA space, **for MNFG**. The  $(i, j)$  scatter plot has principal component  $i$  against principal component  $j$ . The diagonal plots are histograms.

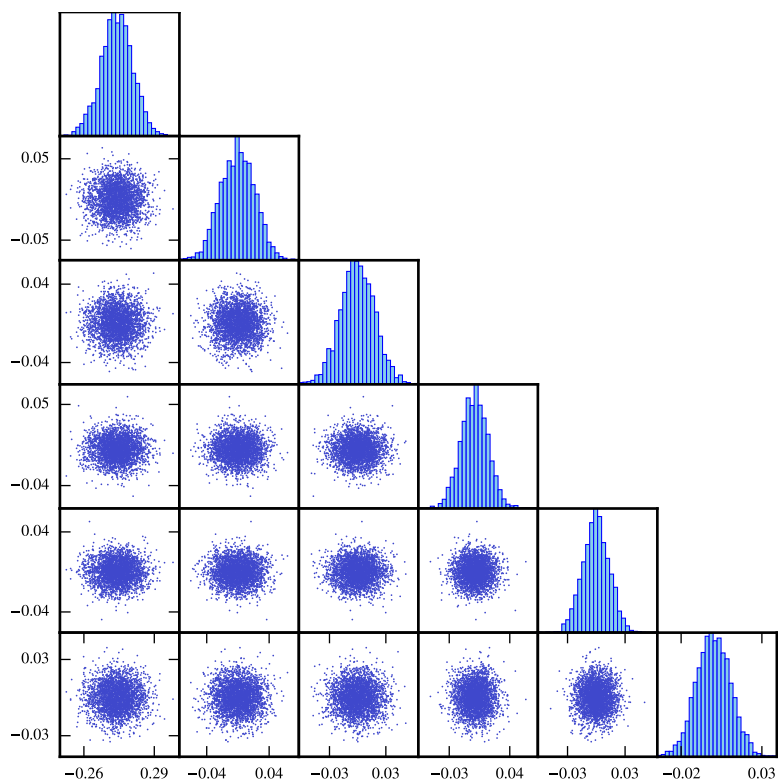


Figure 25: Scatter plots of the generated weights for the entire fourth layer, in PCA space, **for MNFG**. The  $(i, j)$  scatter plot has principal component  $i$  against principal component  $j$ . The diagonal plots are histograms.

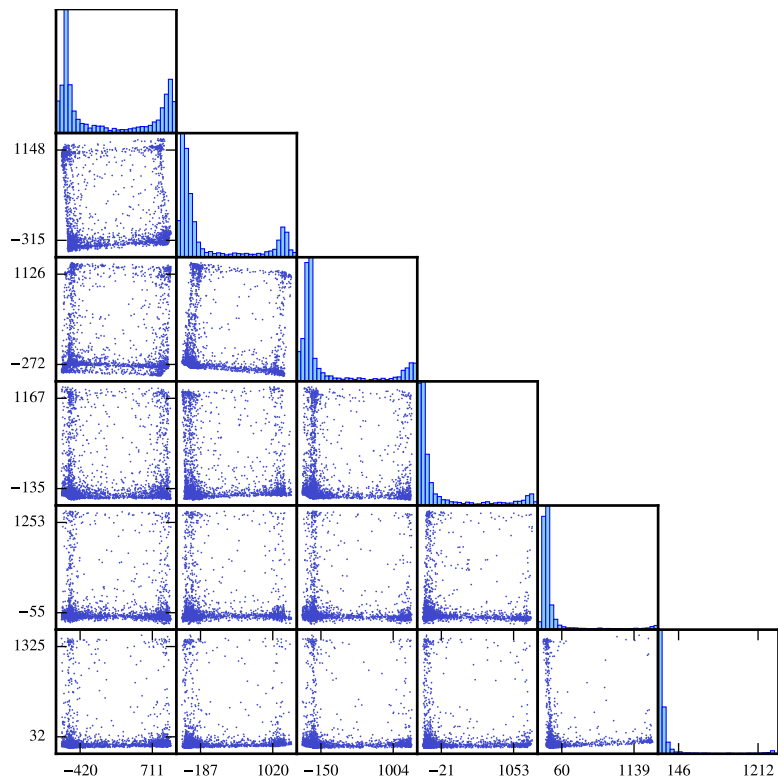


Figure 26: Scatter plots of the generated weights for the entire target network, in PCA space, **for MNFG**. The  $(i, j)$  scatter plot has principal component  $i$  against principal component  $j$ . The diagonal plots are histograms.